A Study on LCoS-Based Remote Nodes for 60 GHz Fiber-Wireless Links

Christina Lim, *Senior Member, IEEE*, Cibby Pulikkaseril, *Member, IEEE*, and Ka-Lun Lee, *Member, IEEE*

***Abstract*—In this paper, we investigate and study the performance of a WDM-based 60 GHz mm-wave fiber-wireless link incorporating a liquid-crystal-on-silicon (LCoS)-based programmable optical processor (POP) in the remote node (RN) for demultiplexing and processing of multiple channels. To ensure that the fiber-wireless link is compatible with existing WDM optical backbones, we have evaluated the performance of the 60 GHz link using a typical WDM channel plan with 100 GHz spacing. A number of different filter profiles are investigated for the POP within the RN and the link performance is quantified and fully characterized. To demonstrate the robustness and flexibility of the POP as a RN, we also investigate wavelength-interleaved 60 GHz fiber-wireless link which requires a more complex filter profile for channel demultiplexing. Our results demonstrate that the POP allows error-free reception of demultiplexed channels, though the performance depends on the type of profile used to process the individual channels.**

***Index Terms*—radio-over-fiber, fiber-wireless, microwave photonics, optical signal processing.**

I. Introduction

Fixed wireless access operating in the millimeter-wave (mm-wave) frequency region with optical fiber backhaul has been actively pursued to provide untethered connectivity for ultra-high bandwidth wireless communications [1-10]. Such wireless networks are able to overcome the spectral congestion in the lower microwave region. The migration to mm-wave frequencies requires the deployment of a pico- or microcellular architecture due to the high propagation losses of signals at these frequencies which, in turn, necessitates a large deployment of functionally simple and compact antenna base stations (BSs) to improve the geographical coverage. Optical fiber backbones are essential in this architecture to provide bandwidth for the transportation of the high-throughput aggregated traffic from all antenna BSs to a central office (CO) where the main signal processing, routing and switching functionalities will be performed.

Manuscript received June 5, 2012. C. Lim is with the Department of Electrical and Electronic Engineering, The University of Melbourne, VIC 3010, Australia. (Phone: +61-3-83444486; fax: +61-3-83447412; e-mail: chrislim@unimelb.edu.au).

C. Pulikkaseril is with Finisar Australia, 224 Young St., Waterloo, NSW 2017, Australia. (e-mail: cibby.pulikkaseril@finisar.com).

K.-L. Lee is with the Department of Electrical and Electronic Engineering, The University of Melbourne, VIC 3010, Australia. (e-mail: alanl@unimelb.edu.au).

This architecture is commonly known as fiber-wireless or radio-over-fiber [1-5]; current deployments of fiber-based infrastructure have ignited interest in the use of optical fiber for wireless backhauling which will further accelerate the development of fiber-wireless systems [8,9].

In addition, there is abundance of bandwidth, especially in the unlicensed 60 GHz band to support extremely high bandwidth wireless signals, and can be combined with spectrally efficient optical networking schemes, such as wavelength division multiplexing (WDM). Fig. 1 shows a typical WDM-based fiber-wireless network where the central office (CO) provides a gateway to the optical WDM backbone while serving a large number of widely distributed antenna base stations (BSs) via remote nodes (RNs). In this architecture, the RN has the basic role of multiplexing/demultiplexing of the multiple WDM fiber-wireless channels before sending back to the CO/distributing to the BSs.

Despite the high-capacity and elegance of the 60 GHz fiber-wireless system, the implementation is not straightforward. Although the optical distribution of wireless signals at 60 GHz is able to simplify the base station design, the transmission distances are limited by RF power fading caused by chromatic dispersion effects in optical fiber [11]. To overcome these impairments in 60 GHz fiber-wireless links, dispersion tolerant schemes such as optical carrier suppression have been widely used [12].

An additional issue is the spectral efficiency of transporting fiber wireless signals, which typically contain an information bandwidth less than 5 GHz, over WDM channels; when using typical channel spacing of 100 GHz, there is a considerable amount of wasted spectrum. A possible solution is to

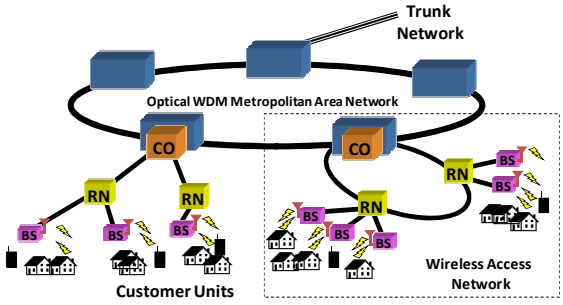

Fig. 1 WDM fiber-wireless network architecture

interleave individual 60 GHz fiber wireless signal together, allowing a greater number of channels to be carried by the link [13,14]. However, this approach requires unconventional optical components to de/multiplex the signals into a single fiber.

Recently, we have proposed and demonstrated an active RN using an LCoS-based programmable optical processor (POP) consolidating the functions of wavelength demultiplexing, optical single sideband with carrier generation and optical carrier suppression for 37.5 GHz fiber-wireless links [15]. In this paper, we further investigate and study the performance of the POP in the RN in a WDM-based 60 GHz fiber-wireless link, where the POP functions as a remotely configurable demultiplexer located in the RN. We study, characterize and quantify the performance of the 60 GHz fiber-wireless link based on the POP configured for operation as a remote node with typical WDM 100 GHz channel spacing. We further evaluate the proposed scheme for more complex channel allocation using wavelength interleaving. The paper is organized as follows. Section II presents our proposed WDM-based 60 GHz fiber-wireless link using POP in the RN for 100 GHz channel spacing and Section III quantifies the crosstalk and link performance for different filter profiles based on 100 GHz channel spacing. Section IV governs the experimental investigation on wavelength interleaved 60 GHz fiber-wireless link with POP in the RN and Section V provides a discussion on the reconfigurability of the POP-based RN, with regards to in-field upgrades of additional channels. Finally Section VI summarizes our proposed schemes and results.

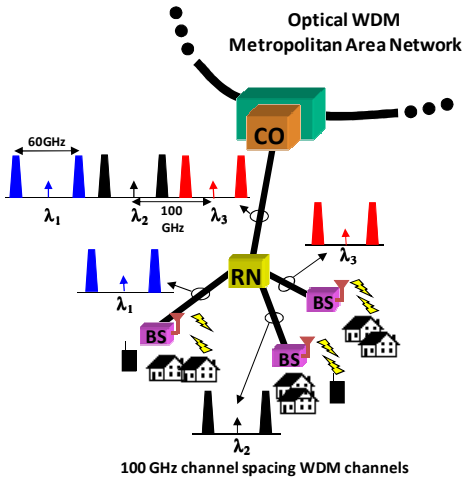

Fig. 2 60 GHz WDM fiber-wireless system with 100 GHz channel spacing

II. Proposed WDM-based 60 GHz Fiber-Wireless Link with 100 GHz Channel Spacing Incorporating a POP in Remote Nodes

As shown in Fig. 1, the basic role of the RN is to demultiplex the downlink WDM channels before distribution to the respective BSs, simultaneously multiplexing the uplink WDM channels back to the CO. Here we propose a reconfigurable RN design using a programmable optical processor capable of demultiplexing WDM channels carrying 60 GHz wireless signals, while additionally performing signal processing functions.

Fig. 2 illustrates the channel allocations for our proposed 60 GHz fiber-wireless arranged to fit within 100 GHz channel spacing. In this study, 2 x 60 GHz wireless signals are externally modulated onto the optical carrier using optical carrier suppression techniques to mitigate the impact of fiber chromatic dispersion on the link performance. At the CO, the 60 GHz fiber-wireless channels are multiplexed together and distributed to the RN. The POP in the RN is programmed to demultiplex these channels before distributing to the respective BSs, and the demultiplexing profiles can be

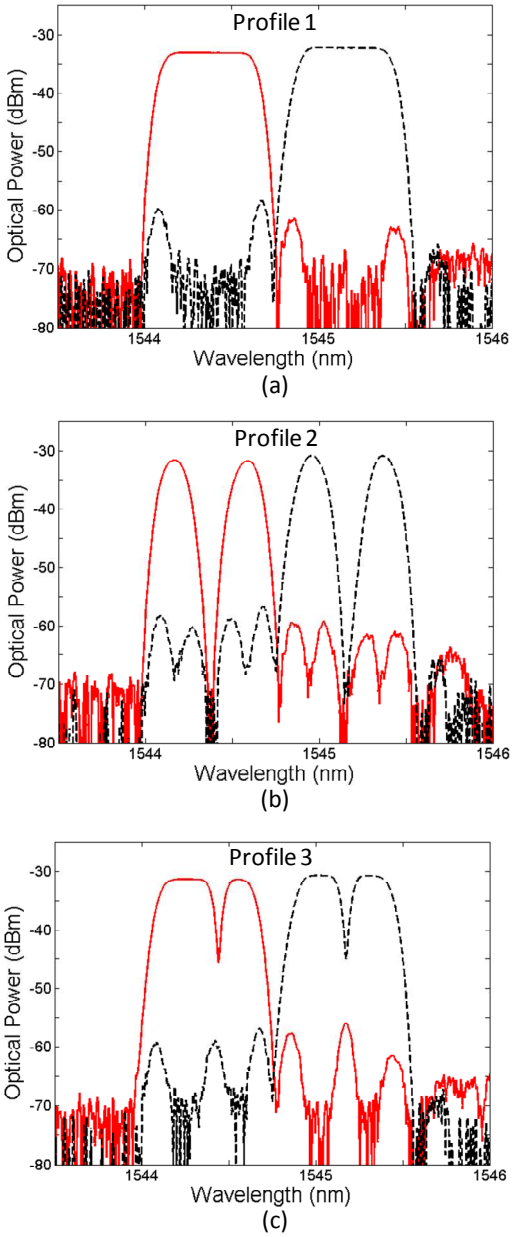

Fig. 3 Filter profiles to be investigated for 60 GHz WDM fiber-wireless links: (a) flattop, (b) flattop with stopband, and (c) flattop with phase notch.

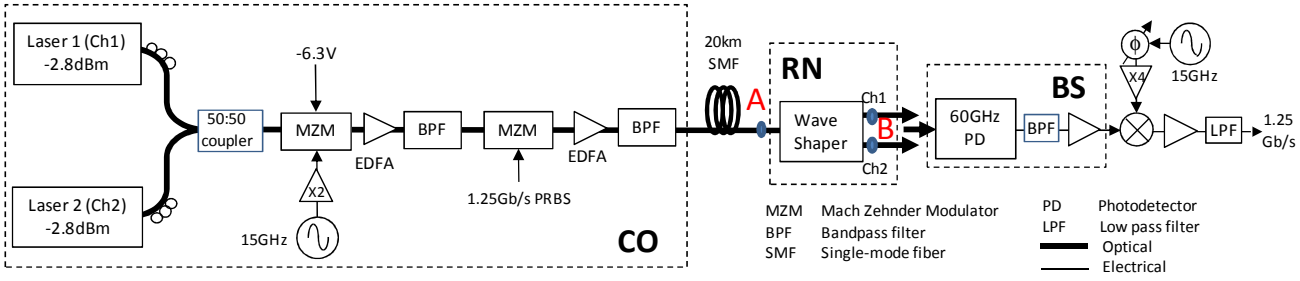

Fig. 4 Experimental setup for 60 GHz fiber-wireless link characterization using programmable optical processor (POP) in RN

customized to perform additional functionality.

In this study, we experimentally investigated the link performance for three different filter profiles configured using the POP: (a) generic flattop bandpass filter, (b) bandpass filter with a stopband at the carrier frequency and (c) bandpass filter with a phase notch at the carrier frequency.

The POP used in our investigation was a Finisar WaveShaper Multiport Optical Processor (4000S). The WaveShaper 4000S is a highly programmable POP based on a 2D array of liquid-crystal-on-silicon (LCoS), allowing arbitrary amplitude and phase shaping over the C-band. This device has a similar optical engine to modern wavelength-selective switches (WSS) based on LCoS technology, which enables reliable, stable operation and switching times less than 100 ms, but also allows amplitude and phase control over the spectrum [16].

Fig. 3a displays the spectral response of the generic flattop filter, with a 3 dB bandwidth of 80 GHz. This was designed to drop the two optical sidebands of the 60 GHz wireless channel (Profile 1) to emulate a typical WDM demultiplexer.

Fig. 3b shows an alternate filter profile which placed a bandstop filter at the carrier frequency, extracting the two sidebands. The resulting bandpass filters had a 3 dB bandwidth of 25 GHz.

Finally, Fig. 3c illustrates the third filter profile, incorporating a phase shift in the middle of the filter band to remove residual optical carrier thus improving the carrier suppression ratio (Profile 3). This was created by setting the relative phase of the left- and right-hand halves of the bandpass filter to have a π phase change.

While the filter profiles shown here were designed for two adjacent channels, it is trivial to configure the POP for a higher channel count, though we acknowledge that the system performance will change at higher channel counts.

To characterize the performance of the 60 GHz fiber-wireless link with the RN configured to these filter profiles, a proof-of-concept fiber-wireless link was constructed, as shown in Fig. 4. In order to analyze the effect of adjacent channel interference, two 60 GHz fiber-wireless signals were generated with 100 GHz spacing. The optical carriers were generated using two tunable lasers tuned to a wavelength of 1544.4 nm (Ch1) and 1545.150 nm (Ch2) respectively with an output power of -2.8 dBm. Both optical carriers were combined using a 3 dB coupler and externally modulated with a 30 GHz RF carrier via a minimum-biased Mach-Zehnder modulator (MZM) to generate 60 GHz optical signals using optical carrier suppression (OCS) technique. Due to the high insertion loss of the MZM, the multiplexed optically modulated 60 GHz signals were amplified using a small-gain Erbium-doped fiber amplifier (EDFA) to compensate for this loss.

The 60 GHz optical signals were then modulated with 1.25 Gb/s wireless data using a pseudo-random pattern generator with a code length of 2^{31}-1 using a 2nd MZM, and subsequently amplified through a 2nd EDFA. The transmitted signals were then propagated through 20 km of single mode fiber (SMF) to the RN. The aggregate optical power before the feeder fiber was +9 dBm. Although OOK data format is used in this demonstration, the proposed active RN is transparent to the wireless data modulation format and hence is able to support current wireless standards.

As discussed earlier, the RN consisted of a single programmable optical processor used to demultiplex the incoming signals using one of the three different filter profiles as shown in Figs. 3a-3c before distribution to the BS. At the BS, the optical channels were detected separately using a 60 GHz Discovery photodetector (PD), amplified, bandpass filtered and downconverted to recover the 1.25 Gb/s data. We note that, though we demonstrate operation using OCS formatted signals, the POP is easily reconfigured to handle other modulation schemes in a radio-over-fiber platform.

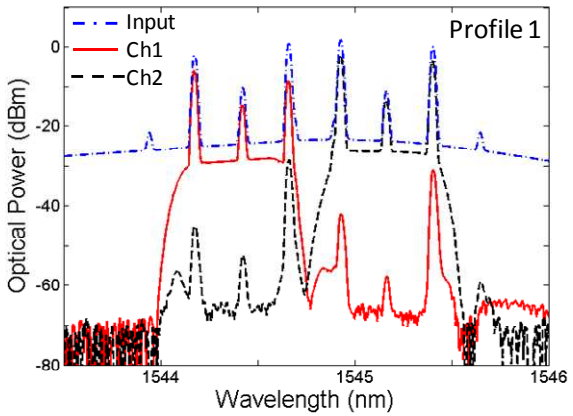

Fig. 5 Measured optical spectra before and after RN for filter profile 1

III. Experimental Results and Crosstalk Characterization for 100 GHz Channel Spacing

To quantify the performance of the POP-based RN in a 60 GHz fiber-wireless link, we used the experimental setup in Fig. 4, with the POP configured with one of the three filter profiles shown in Figs. 3a-3c.

A. Simple bandpass filter

Fig. 5 displays the measured optical spectra before (point A in Fig. 4) and after (point B in Fig. 4) the RN, where the profile set on the POP corresponds to profile 1 (Fig. 3a). As can be seen from the results, the two channels can be successfully demultiplexed using filter profile 1 with crosstalk greater than 20 dB for both channels, and out-of-band noise suppressed to more than 30 dB.

One of the Ch1 sidebands has been attenuated by the demultiplexing function of the POP, which degrades the performance of the link. In this case, the coarse tuning resolution of the tunable laser limits the alignment of the carrier wavelength to the center of the passband. However, lasers used for WDM networks would be tightly locked to the ITU grid, which ensures that both sidebands to be transmitted evenly.

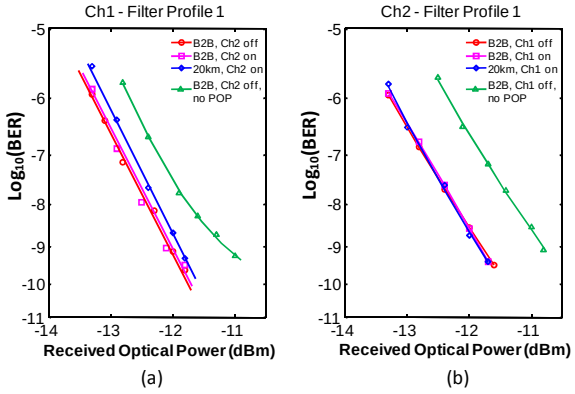

Fig. 6 Measured BER curves (a) Ch1 and (b) Ch2 with RN programmed with filter profile 1

The measured bit-error-rates (BER) for both channels (Ch1 and Ch2) are shown in Fig. 6a and 6b, respectively. The BERs were measured for back-to-back (B2B) and transmission over 20 km of SMF. To quantify the crosstalk between channels, the BER was also measured with and without the adjacent channel. The results show that there is negligible crosstalk between the channels and both channels are successfully recovered after transmission over 20 km of SMF with minimal penalty. For comparison, we have also measured the BER for each channel without the POP-based RN in the link and without the adjacent channel. The results are also plotted in Figs. 6a and 6b. It can be seen that without the POP, the link incurred an additional power penalty of ~1 dB to achieve a BER = 10^{-9}.

B. Bandpass filter with stopband for carrier removal

Fig. 7 shows the measured optical spectra before and after the RN (Point A and B in Fig. 4) when the POP was configured with profile 2 (Fig. 3b). The two adjacent channels

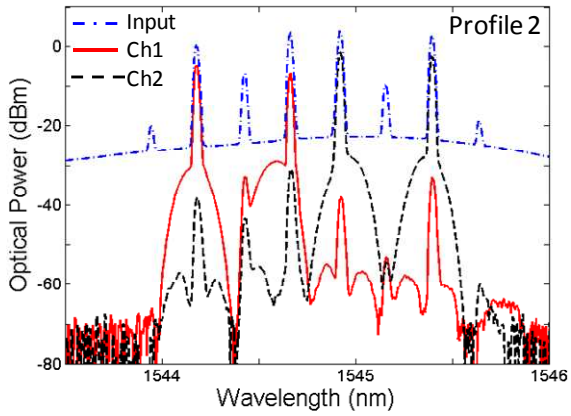

Fig. 7 Measured optical spectra before and after RN for filter profile 2

are successfully demultiplexed with similar levels of crosstalk to profile 1; however, the attempt to suppress the carrier with a stopband also removes much of the in-band noise.

We observe from Fig. 7 that the carrier of channel 2 is much better suppressed compared to channel 1, demonstrating a particular limitation of the POP. Though it is a versatile component in the RN, the relatively coarse resolution of the POP does not guarantee that narrow spectral features can be arbitrarily manipulated. In this case, finer tunability on the optical source would aid in achieving high suppression of the carrier.

Figs. 8a and 8b show the measured BER for back-to-back (with and without adjacent channel) and 20 km SMF transmission for Ch1 and Ch2 respectively. Results also show that there is minimal crosstalk between channels and negligible penalty after transmission over 20 km of SMF.

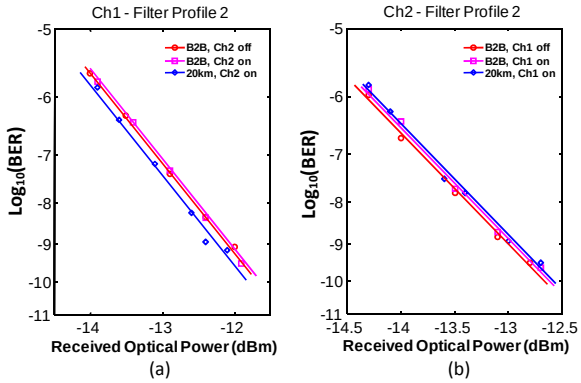

Fig. 8 Measured BER curves (a) Ch1 and (b) Ch2 with RN programmed with filter profile 2

C. Bandpass filter with notch filter for carrier removal

We repeat the performance investigation using filter profile 3 (Fig. 3c) and shown in Fig. 9 are the measured optical spectra before and after the RN (Point A and B in Fig. 4).

This filter profile uses a π phase change in the center of the passband to create an extremely narrow notch filter, with the aim of completely suppressing the optical carrier, thereby improving the modulation depth of the fiber-wireless signal. It can be seen from Fig. 9 that the optical carrier for both channels are completely suppressed (> 25 dB suppression). Similar sideband attenuation is observed for Ch1 as for the

case for filter profiles 1 and 2. The crosstalk isolation and out-of-band noise rejection were similar to the previous filter profiles.

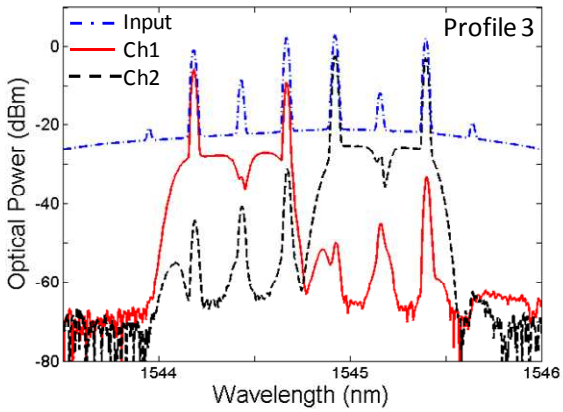

Fig. 9 Measured optical spectra before and after RN for filter profile 3

The BERs for the link were measured for B2B (with and without adjacent channel) and 20 km of SMF transmission, with results plotted in Figs. 10a and 10b for Ch1 and Ch2 respectively. Again, there is negligible crosstalk between channels and minimal power penalty for transmission over 20 km of feeder fiber.

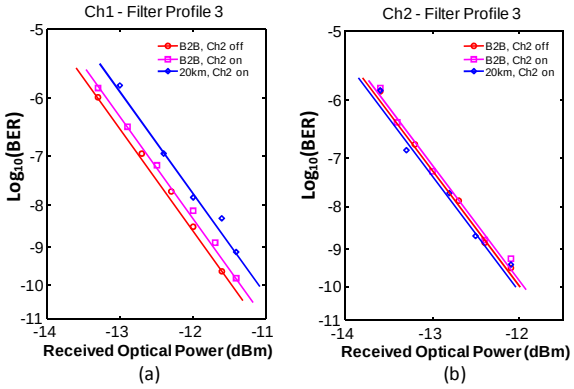

Fig. 10 Measured BER curves (a) Ch1 and (b) Ch2 with RN programmed with filter profile 3

D. Discussions

Fig. 11 summarizes the experimental results for the 60 GHz fiber-wireless link based on 100 GHz channel spacing using a POP with different filter profiles at the RN. Looking at Ch2 (Fig. 11b), we can see that the best link performance in this study is when the POP-based RN is configured with profile 2, while profile 1 has the worst performance.

Filter profile 2 removes more in-band noise compared to profiles 1 and 3, which results in the superior link performance. However, the passbands carrying the modulated optical signals are rounded due to the limitation of the optical imaging system in the POP. While this may be negligible for the data rate measured here (1.25 Gb/s), as the requirement on modulation bandwidth increases, this filter profile may suffer penalties.

In comparison, filter profile 3 passes more in-band noise than profile 2, justifying the degraded link performance. However, the benefit of the profile 3 is that the narrowband notch filter allows a wider, flatter passband for the modulated optical signals. If this fiber-wireless link is to be upgraded to higher data rates, filter profile 3 provides the response to handle large modulation bandwidths. Additionally, we note that a reconfigurable RN allows the system operator to select the optimum profile based on the requirements of the link.

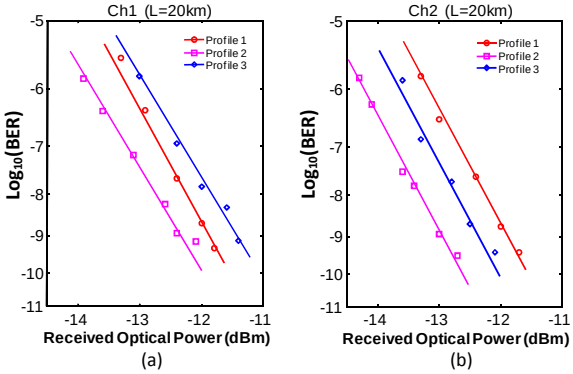

Fig. 11 Comparison of BER curves for all filter profiles for transmission over 20 km of SMF for (a) Ch1 and (b) Ch2

Similarly Ch1 (Fig. 11a) also exhibits the best link performance with filter profile 2. However, we observe that the performance of Ch1 suffers an additional penalty as compared to Ch2, which is attributed to the power imbalance between the two modulated sidebands. This demonstrates the importance of aligning the channel center to the laser peak frequency. Nevertheless, error-free transmission is still achievable for all filter profiles investigated.

From this investigation, it can be seen that by incorporating a POP within the RN of a WDM-based 60 GHz fiber-wireless link with standard 100 GHz channel spacing, we are able to configure the POP dynamically to match the link performance specifications. The POP can be programmed not only as a demultiplexer with reconfigurable filter profiles and also optically process the signal if required. Our studies show that different filter profiles have an impact on the performance of the link up to 1 dB improvement in certain cases.

IV. Experimental Results for Wavelength-Interleaved 60 GHz Fiber-Wireless Link with Active Remote Node

In this section, we investigate the performance of the 60 GHz fiber-wireless link in a more complex channel allocation and study how the POP can improve the RN architecture. As discussed earlier, using a standard DWDM channel plan for fiber-wireless links results in excessive spectral inefficiency, as the information bandwidth of each fiber-wireless channel is substantially less than the 100 GHz DWDM channel. One proposed solution to improving spectral efficiency is to introduce a wavelength-interleaving scheme that weaves the fiber-wireless sidebands among each other, maximizing the number of channels that the spectrum is able to carry [13,14].

The channel allocation is illustrated in Fig. 12, where the 60 GHz fiber-wireless optical signals are interleaved with the

adjacent channels as such that the channel spacing is reduced to 40 GHz. The RN is required to demultiplex the complex channel allocation before distributing the signals to respective base stations. In most cases, a number of custom-designed fiber Bragg gratings (FBGs) with two notches corresponding to the channel sidebands are required within the RN to drop and add the channels. This design is extremely inflexible and also impedes future link upgrades. To overcome this, we propose using the POP-based RN to offer a reconfigurable solution to perform wavelength interleaving. The POP is programmed with the appropriate filter profiles to demultiplex or multiplex the interleaved fiber-wireless channels.

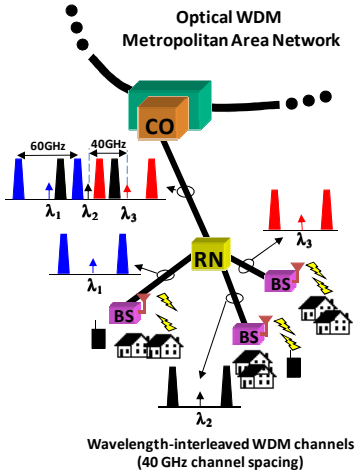

Fig. 12 60 GHz WDM fiber-wireless system incorporating wavelength interleaved scheme to improve spectral usage

To demonstrate our proposed scheme of using a POP in the RN to demultiplex wavelength interleaved 60 GHz fiber-wireless channels, we used the same experimental setup in Fig. 4 and programmed the WaveShaper to have the filter profile shown in Fig. 13a. The filter profile for each channel consists of two passbands of 25 GHz separated by 60 GHz in order to extract the two sidebands of the 60 GHz fiber-wireless signal. As can be seen from Fig. 13a, due to the densely packed interleaved channels, the filter profiles for the interleaved channels are also closely packed and overlap with that of the adjacent channels. To investigate the performance of the link with such filter profiles, two optical channels at 1544.4 nm (Ch1) and 1544.762 nm (Ch2) were used to generate the 60 GHz fiber-wireless signals in optical carrier suppressed modulation format. The measured optical spectra before and after the RN (WaveShaper) are shown in Fig. 13b. The crosstalk level between the two adjacent channels as a result of the profile crossover is as high as 20 dB relative to the desired channel. In addition, the signal insertion loss for this profile is ~10 dB and approximately 6 dB higher compared to the profiles investigated in Section III.

We have measured the BERs for B2B (with and without adjacent channels) and also transmission over 20 km of SMF and the results are shown in Figs. 14a and 14b for Ch1 and Ch2 respectively. It can be seen that there is no significant crosstalk penalty between the channels with a maximum of 0.35 dB for Ch1. Similarly there is negligible power penalty (<0.5 dB) for transmission over 20 km of SMF for both channels. These results indicate that despite the complex channel allocations to improve spectral efficiency of the 60 GHz fiber-wireless link, the active RN incorporating the POP is able to successfully demultiplex the fiber-wireless channels simultaneously with error-free transmission. Such configuration is attractive and able to overcome the needs for

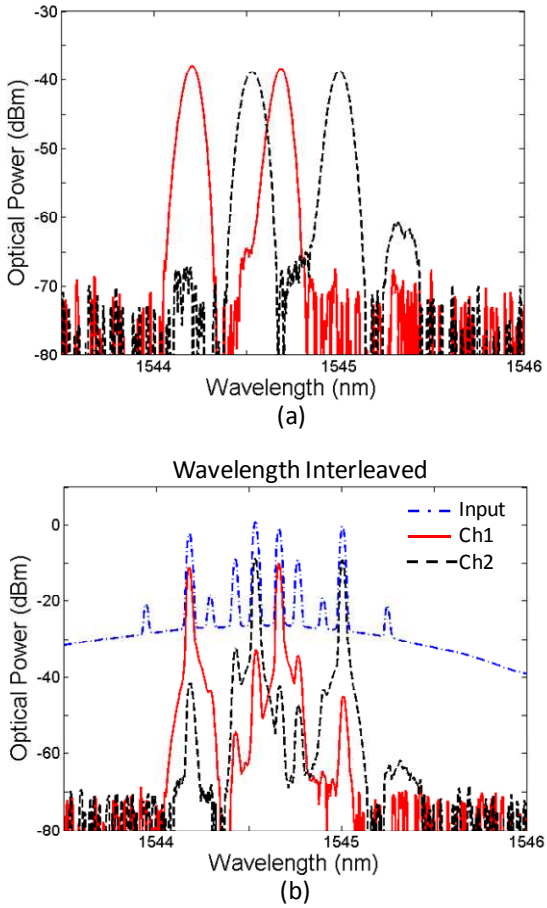

Fig. 13 (a) Measured filter profile for demultiplexing interleaved channels (b) Measured optical spectra before and after RN for wavelength interleaved 60 GHz fiber-wireless link

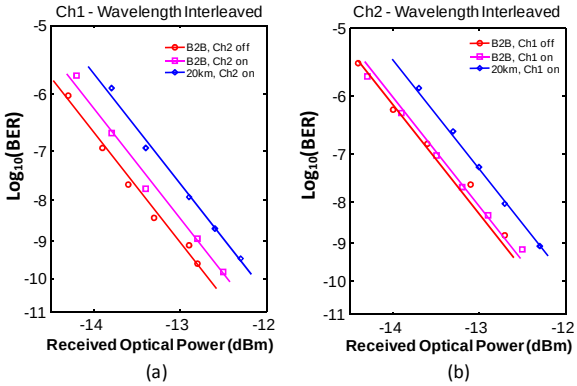

Fig. 14 Measured BER curves for (a) Ch1 and (b) Ch2 for wavelength interleaved channel allocation

custom-designed FBGs for each channel while maintaining flexibility, robustness and ease-of-upgrade features.

V. Upgradability and Flexibility of Using POP in Fiber-Wireless RN

In Section III-D, we observed that filter profile 2 (using a stopband in the center of the DWDM channel) led to the best link performance. However, we hypothesized that filter profile 3 (using a notch filter in the center of the passband) may support larger modulation bandwidths for future link requirements. This highlights an important feature of moving to a reconfigurable RN; as the demands of the network continue to grow, the POP can be remotely configured to add channels.

The nonlinear behavior of optical amplifiers in the network makes it difficult to simply add channels, however. Once the system has been optimized for a given channel plan, additional channels will impact the gain seen by each channel, as well as the out-of-band noise that accumulates in the system. Equalization schemes for these effects have been documented extensively [17], but we propose to consolidate this effect into our reconfigurable RN.

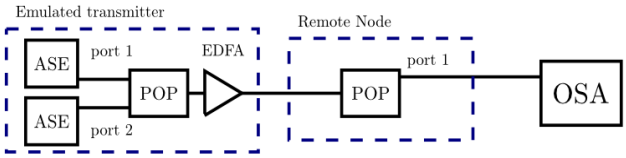

Fig. 15 Experimental setup to demonstrate reconfigurability and dynamic functionality of the POP-based RN.

To demonstrate this concept, we assembled a simplified experiment, where our goal is simply to demonstrate the ability of the POP-based RN to be reconfigured with additional channels, as well as performing gain equalization.

Fig. 15 outlines our setup; to emulate the creation of a large number of channels, we elected to use the POP to carve amplified spontaneous emission noise (ASE) spectra into our desired channel plan. We insert ASE into ports 1 and 2 of the POP, and use filter profile 3 (Fig. 3c), with a phase notch in the center of the passband, extended to 25 channels starting from 193.2 THz, with 100 GHz spacing. An optical amplifier is used to boost the power of channels prior to deployment; at the receiver end, the reconfigurable RN uses a POP to demultiplex the channels. At this point, the channel powers exiting the RN are unbalanced due to the gain response of the EDFA.

Fig. 16 displays the emulated channel plan exiting the transmitter section, with 25 channels spaced 100 GHz apart, with a clear power variation over the channels. The RN performs demultiplexing, but also adds additional attenuation to ensure that the channel powers exiting the RN are relatively well balanced. This considerably simplifies the BS design by eliminating the need for power equalization before photodetection.

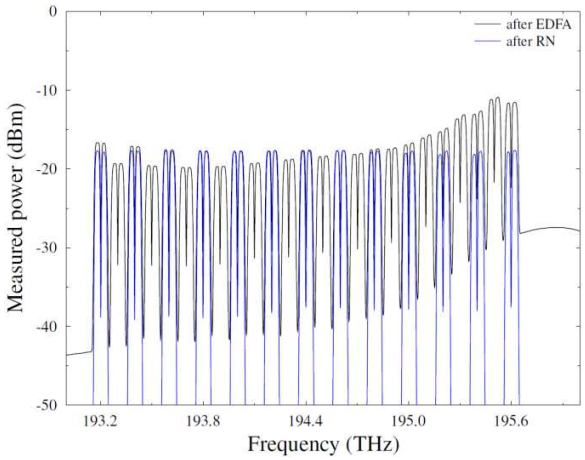

Fig. 16 Gain flattening and demultiplexing 60 GHz fiber-wireless channels in the POP-based RN.

The POP-based RN allows for in-field upgrades to the channel plan by remote configuration, but, similarly, this can disturb the power balancing in the spectrum. Fig. 17a displays the initial output of port 1, with 13 (out of an original 25) balanced 60 GHz fiber-wireless channels exiting one port of the RN. Upon the upgrade to 40 channels, however, the power variation between channels increases to as much as 5 dB, which may cause a failure at selected BS (Fig. 17b).

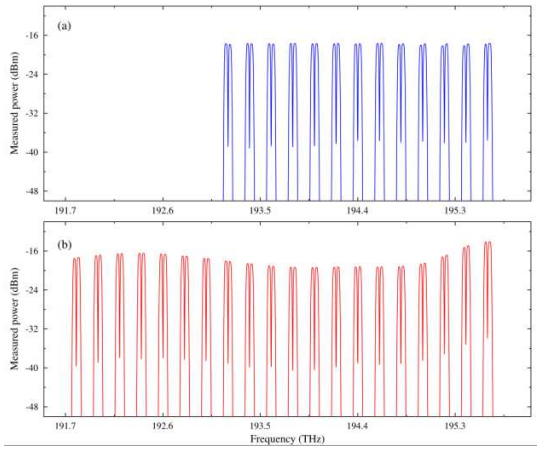

Fig. 17 The impact of channel plan upgrades on the demultiplexed output of the POP-based RN. Initially, (a) channels are well balanced, but (b) poorly balanced upon the addition of 15 more channels.

The flattening process is carried out again producing a well balanced channel plan, shown in Fig. 18. This flattening process is simple to implement and can be automated in a feedback loop, using a channel monitor to produce the error signal. The LCoS-based POP is able to update at roughly 3 Hz, which should be sufficient for gain equalization. As observed from Fig. 18, the notch filters at the center of the passband are still evident, demonstrating that the addition of attenuation to the POP does not significantly disturb the relative phase relationship on the LCoS.

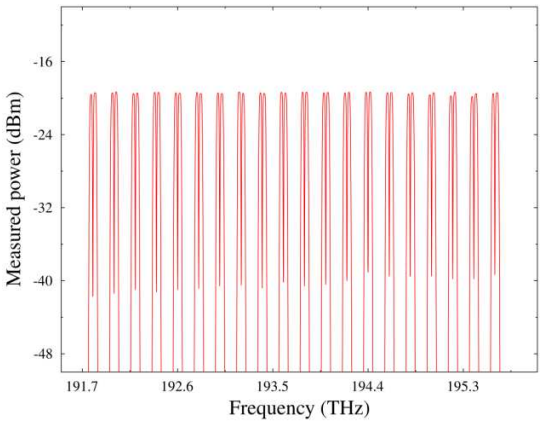

Fig. 18 Gain flattening at the RN after a channel upgrade from 25 to 40 channels.

VI. CONCLUSIONS

We have proposed and studied the design for the RN of a 60 GHz WDM fiber-wireless system based on a POP for wavelength demultiplexing and signal processing. In this investigation, we have studied WDM-based 60 GHz fiber-wireless link with 100 GHz channel spacing to ensure compatibility with existing WDM infrastructure. To demonstrate the capability and robustness of the POP based RN, three different filter profiles were thoroughly studied with crosstalk and link performance quantified. Due to the high-isolation of the filter profiles generated using the POP, minimal crosstalk was observed for all cases investigated. Based on our investigation, the performance of the 60 GHz fiber-wireless link based on 100 GHz channel spacing can be enhanced by modifying the filter profile to improve the signal-to-noise ratio.

We have also investigated the link performance for more complex channel allocations such as using the wavelength-interleaved scheme. Our results show that the POP in the RN can simultaneously demultiplex the interleaved channels with error-free transmission. Our proposed POP-based RN for 60 GHz fiber-wireless links is very flexible, robust and enables simple future system upgrades.

REFERENCES

[1] J. Capmany and D. Novak, "Microwave photonics combines two worlds," *Nature Photonics*, vol. 1, pp. 319-330, 2007.

[2] D. Novak, A. Nirmalathas, C. Lim, and R. Waterhouse, "Fibre Radio Technology", in *Microwave Photonics: Devices and Applications;* ed. Stavros Iezekiel, John Wiley & Sons, Ltd., London UK, pp. 169-190, 2009.

[3] H. Ogawa, "Millimeter-wave wireless personal network systems," *Proc. IEEE Radio Frequency Integrated Circuits (RFIC) Symposium*, Jun. 2006.

[4] C. Lim, A. Nirmalathas, M. Bakaul, P. Gamage, K.-L. Lee, Y. Yang, D. Novak, and R. Waterhouse, "Fiber-wireless networks and subsystem technologies," *IEEE Journal of Lightwave Technology*, vol. 28, no. 4, pp. 390-405, Feb. 2010.

[5] B. Cabon and Y. Le Guennec, "Recent progresses in fiber-wireless systems," *Proc. LEOS Annual Meeting 2009*, pp. 608-609.

[6] M. Sauer, A. Kobyakov, J. George, "Radio over fiber for picocellular network architectures," *JLT*, vol. 25, no. 11, pp. 3301-3320, November 2007.

[7] A. Ng'oma and M. Sauer, "Opportunities and challenges in optical generation and distribution of 60 GHz wireless signals," *Proc. Asia Pacific Microwave Conference 2008*, pp. 1-4.

[8] Y. Luo, T. Wang, S. Weinstein, M. Cvijetic, and S. Nakamura, "Integrating optical and wireless services in the access network," *Proc. OFC 2006*, paper NThG1, 2006.

[9] G. Shen, R.S. Tucker, and C.-J. Chae, "Fixed mobile convergence architectures for broadband access: integration of EPON and WiMAX," *IEEE Comm. Mag*., pp. 44–50, Aug. 2007.

[10] S. T. Choi, K S. Yang, S. Nishi, S. Shimizu, K. Tokuda, and Y. H. Kim, "A 60 GHz point-to-multipoint millimeter wave fiber-radio communication system," *IEEE Trans. on MTT*, vol. 54, no. 5, pp. 1953-1959, May 2006.

[11] H. Schmuck, "Comparison of optical millimeter-wave system concepts with regard to chromatic dispersion," *Electron. Lett.*, vol. 31, no. 21, pp. 1848-1849, 1995.

[12] S-H. Fan, H-C Chien, Y-T Hsueh, A. Chowdhury, J. Yu, and G-K. Chang, "Simultaneous transmission of wireless and wireline services using a single 60-GHz radio-over-fiber channel by coherent subcarrier modulation," *IEEE Photon. Technol. Lett.*, vol. 21, no. 16, pp. 1127-1129, 2009.

[13] C. Lim, A. Nirmalathas, D. Novak, R.S. Tucker, and R.B. Waterhouse, "Technique for increasing optical spectral efficiency in millimeter-wave WDM fibre-radio", *IEE Electronics Letters*, Vol. 37, No. 16, pp. 1043-1045, Aug. 2001.

[14] H. Toda, T. Yamashita, K. Kitayama, and T. Kuri, "A DWDM mm-wave fiber-radio system using optical interleaving for high spectral efficiency," *Proc. Microwave Photonics 2001*, pp. 85-88.

[15] C. Lim, C. Pulikkaseril, K.L. Lee, A. Nirmalathas, and M. Roelens, "Consolidation of signal processing functions in WDM-based mm-wave fiber wireless links using a LCoS-based programmable optical processor", *Proc. 2010 IEEE Microwave Photonics (MWP2010)*, Montreal, Canada, pp. 58-61, Oct 2010.

[16] M. Roelens, S. Frisken, J. Bolger, D. Abakoumov, G. Baxter, S. Poole, and B. Eggleton, "Dispersion trimming in a reconfigurable wavelength selective switch," *J. Lightwave Technol*., vol. 26, pp. 73-78, 2008.

[17] M. Rochette, M. Guy, S. LaRochelle, J. Lauzon, and F. Trepanier, "Gain equalization of EDFA's with Bragg gratings," *IEEE Photon. Technol. Lett.*, vol. 11, no. 5, pp. 536-538, 1999.